

# Mobile Sensors Deployment Subject to Measurement Error

Hamid Mahboubi, Mojtaba Vaezi, and Fabrice Labeau

Department of Electrical and Computer Engineering  
McGill University, Montreal, Quebec H3A 0A9, Canada

**Abstract**—Single-cell-based coverage hole detection algorithms are developed for mobile sensors deployment under inaccurate location information and non-identical sensing ranges. Existing Voronoi-based diagrams require the exact location of sensors to guarantee a simple, single-cell-based coverage detection, and they miss the mark if the location information is inaccurate. The guaranteed Voronoi-based diagrams, proposed in this paper, extend the existing diagrams in a way to guarantee the single-cell based coverage hole detection when upper bounds on location errors are provided. Simulation results show that with inaccurate location information the proposed algorithms can largely increase the network coverage. Even if the location information is exactly known, we suggest assuming some error margins to improve the network coverage based on the proposed algorithms.

## I. INTRODUCTION

Fulfilling the sensing tasks in wireless sensor networks crucially depends on sensing coverage of sensor nodes. Mobile sensors are used to provide the required coverage by moving toward the correct places. *Distributed* deployment of mobile sensors is preferred to the *centralized* one, in certain circumstances. Movement-assisted sensor deployment protocols are designed to reduce the coverage holes; *Voronoi diagrams* [1]–[4] are popular to discover the coverage holes. For a set of sensors, a Voronoi diagram partitions the space into polygons in a sense that every point in a given polygon is closer to the sensor in that polygon than to any other sensor. This facilitates finding the coverage holes as in each polygon any point out of the sensing range of the corresponding sensor will be a coverage hole. A new type of network to address the coverage and connectivity problems simultaneously is proposed in [5]. An adaptive deployment algorithm called ATRI is proposed in [6] to minimize coverage gaps and maximize coverage area in an unattended mobile sensor networks. The authors in [7] developed an energy-efficient algorithm in a network of heterogeneous mobile sensors. In [8] an algorithm is proposed to cover a sensing field while minimizing the moving distance of sensors.

The Voronoi-based sensor deployment, introduced in [1], assumes that the sensing radii of sensors are the same and the exact positions of sensors are known by every sensor. When the sensing radii of the sensors are different, a point in one polygon may be covered by a sensor in a neighboring polygon while it is not covered by its own sensor. Therefore, to find a coverage hole one needs to compute its distance to the sensor belonging to that polygon as well as all neighboring sensors. Different variants of the Voronoi diagram,

collectively known as *Weighted Voronoi diagram*, are then proposed to overcome this shortcoming [9].

The aforementioned Voronoi diagrams, and corresponding deployment algorithms, are however based on the assumption that the exact location of all sensors are known. In practice, however, each sensor measures the position of its neighboring sensors by using a localization technique [10] or it receives the location information by communication with them via a noisy communication channel. That is, the locations of neighboring sensors are not exact and this problem is still challenging as the performance of the system depends on the accuracy of the sensors' position.

In this paper we study non-identical mobile sensor networks where sensors' locations are inaccurate as they are subject to measurement errors. Assuming upper bounds for the errors, we develop two Voronoi-based diagrams that can be used to find coverage holes in a cell-based approach. We then apply these diagrams to sensor deployment algorithms that use farthest point and minmax point strategies for sensor movement. The proposed algorithms can be applied for both cases when the location information is accurate and inaccurate.

The rest of the paper is organized as follows. To get a better understanding of the Voronoi-based diagrams, we review them in Section II; this sets the stage to propose guaranteed Voronoi-based diagrams in Section III. Then we use the proposed diagrams for sensor deployment in Section IV. Numerical results in Section V confirm the merit of the proposed algorithms to the existing ones. This is followed by our concluding remarks in Section VI.

## II. VORONOI DIAGRAMS IN SENSOR DEPLOYMENT

In mathematics, a *Voronoi diagram* or Voronoi partition of a collection of points (called seeds, nodes, etc.) is a partition of a plane into cells (polygons) each of which contains exactly one node and every point in a given polygon is closer to its generating node than to any other node. Voronoi diagrams are popular in discovering the coverage holes in sensor deployment algorithms.

In this paper we consider a field  $\mathcal{F} \subset \mathbb{R}^2$  containing  $n$  sensors  $s_i$ ,  $1 \leq i \leq n$ , with sensing ranges  $r_i$ ,  $r_i > 0$ , located at distinct positions  $p_i$ . We denote this set by  $\mathcal{S} = \{s_i\}$ , where  $i \in \mathcal{N} := \{1, 2, \dots, n\}$ . Throughout this paper  $i, j \in \mathcal{N}$  and unless otherwise stated  $i \neq j$ .

### A. Identical Sensors

Consider a set of identical sensors with the same sensing radii, i.e.,  $r_i = r_j = r$ . The *Voronoi diagram (VD)* partitions the field into  $n$  subregions, each of which corresponding to one of the sensors, such that it is guaranteed that if a point is not sensed by its corresponding sensor, no other sensor can sense it either. More precisely, assuming the same sensing radius for all sensors, the region corresponding to sensor  $i$  is defined by

$$\Pi_i^{\text{VD}} = \{q \in \mathcal{F} \mid d(q, p_i) \leq d(q, p_j)\}, \quad (1)$$

where  $d(x, y)$  denotes the *Euclidean distance* between two points  $x$  and  $y$ .

Obviously, if  $s_i$  is not able to sense a given point  $q$  in its own region, i.e., if  $d(q, p_i) > r_i$ , then other sensors are not able to do so, either. Hence, to find the coverage holes of the field  $\mathcal{F}$ , it suffices to check the coverage holes at each cell individually. This idea simplifies finding the coverage holes at a sensor network; it is, thus, used to develop self-deployment protocols for sensor networks [1].

### B. Non-Identical Sensors

The above partitioning is based on the assumption that the sensing ranges of the sensors are equal, i.e.,  $r_i = r_j = r$ . When the sensing radii of the sensors are different, the partitioning introduced in (1) no longer implies that coverage holes can be found individually in each cell, since a point that is not covered by the sensor belonging to its own polygon can be covered by neighboring sensors. Weighted forms of the Voronoi diagram, in which the distances are defined by some common metrics modified by weights assigned to generator nodes, are used to overcome this drawback. Here we review two of them.

1) *Multiplicatively Weighted Voronoi Diagram (MWVD)*: This diagram is developed based on multiplying the distance between points by positive weights [11]. In the context of sensor deployment, the multiplicatively weighted distance of a point  $q$  from the sensor  $(s_i, r_i)$  is usually defined as  $d_{\text{MW}}(q, s_i) := \frac{1}{r_i} \times d(q, p_i)$ , where  $p_i$  represents the position of  $s_i$ .

Using the above weighted distance, the set of all points  $q$  which are closer to the sensor  $s_i$  than to any other sensor, in the field  $\mathcal{F}$ , is characterized by

$$\Pi_i^{\text{MWVD}} = \{q \in \mathcal{F} \mid \frac{d(q, p_i)}{r_i} \leq \frac{d(q, p_j)}{r_j}\}. \quad (2)$$

2) *Power Diagram (PD)*: A power diagram partitions the field of sensors based on a somewhat different criterion, i.e., the power of points with respect to the sensing circumference of the sensors [12]. In computational geometry, the power of  $q$  with respect to a circle of radius  $r_i$  centered at  $p_i$  is defined as  $d_p(q, s_i) = d^2(q, p_i) - r_i^2$ ,<sup>1</sup> and the subregion corresponding to  $s_i$  is characterized by

$$\Pi_i^{\text{PD}} = \{q \in \mathcal{F} \mid d^2(q, p_i) - r_i^2 \leq d^2(q, p_j) - r_j^2\}. \quad (3)$$

<sup>1</sup>Then, points outside the sensing area of  $s_i$  have positive power and points inside that have negative power.

The power diagram may be also seen as a weighted form of the Voronoi diagram considering each sensor's squared radius as a weight that is subtracted from the squared distance.

*Remark 1.* From (1)–(3), it is easy to see that when  $r_i = r_j$  for all  $i, j \in \mathcal{N}$ , the above weighted Voronoi diagrams (MWVD and power diagram) reduce to the Voronoi diagram.

The following proposition states a common property of the above diagrams, which is basically one of the most important properties of them as well.

**Proposition 1.** *For both weighted Voronoi diagrams represented by (2)–(3),  $d(q, p_i) > r_i$  implies that  $d(q, p_j) > r_j$ , for any  $q \in \Pi_i$ . Therefore, if a point in one cell is not covered by its corresponding sensor it cannot be covered by any other sensor [9]. Therefore, the coverage holes can be found based on single cell investigations.*

The Voronoi-based diagrams discussed in this section work well if the perfect locations of all sensors are available at every sensor; otherwise, the cells defined by (1)–(3) are not exact and consequently the single-cell-based search fails to find the coverage holes correctly since Proposition 1 does not necessarily hold. In addition, the coverage holes are no longer reliable. In the following, we generalize the above diagrams for imperfect location information.

## III. GUARANTEED VORONOI-BASED DIAGRAMS

In a real-world sensor network, communication between the sensors is subject to errors and other imperfections. Therefore, even if each sensor perfectly knows its own position the other sensors may not have this information perfectly. This is correct even if the sensors' positions are broadcasted through a central unit. Furthermore, each sensor may estimate the position of its neighboring sensors by using a localization technique, rather than receiving it via communication with other sensors or a central unit. In any case, if the users cannot obtain the accurate location information, the related applications, e.g., coverage hole detection, cannot be accomplished. These motivate investigation of methods that guarantee a cell-based coverage analysis, given inaccurate location information.

We study a sensor network in which the positions of sensors are measured, or received via a noisy link, and thus are subject to errors. We assume measurement errors are upper bounded and these bounds are known at each sensor. More precisely,  $p_i$  (the exact location of  $s_i$ ) is assumed to be within a disk of radius  $\epsilon_{ij}$ ,  $\epsilon_{ij} \geq 0$ , centered at  $p_{ij}$  (the measured position of  $i$ th sensor at sensor  $j$ ). Hence,  $d(q, p_{ij}) - \epsilon_{ij} \leq d(q, p_i) \leq d(q, p_{ij}) + \epsilon_{ij}$ . We further assume that each sensor  $s_i$ , measures its own location with some error; this is represented by  $p_{ii}$  and the error bound is assumed to be  $\epsilon_{ii}$ . Our objective is to find  $n$  subregions, each corresponding to one of the  $n$  sensors, such that it is guaranteed that if a point inside a subregion is not sensed by its corresponding sensor, no other sensor can sense it

either. With this in mind, in what follows, we generalize the existing Voronoi diagrams; these are named guaranteed Voronoi diagrams.

### A. Regions' Characteristics

Here, we modify the cell partitioning algorithms in a way that, even in the presence of measurement errors, a single-cell-based search for coverage holes is guaranteed within each cell. To this end, we design the cell borders based on the worst case scenario. That is, we use  $d(q, p_{ii}) + \epsilon_{ii}$  and  $d(q, p_{ij}) - \epsilon_{ij}$ , rather than  $d(q, p_i)$  and  $d(q, p_j)$  when finding the cell borders. This means that, at the worst case where sensor  $s_i$  is shifted  $\epsilon_{ii}$  away from point  $q$  in its region and the neighboring sensors have moved toward  $q$  by maximum amount of error  $\epsilon_{ij}$ , still the  $i$ th sensor is closer to  $q$  than any neighboring sensors.

Then, the mathematical characterization of the  $i$ th region for different diagrams can be modified as below:

#### 1) Guaranteed MWVD (GMWVD):

$$\Pi_i^{\text{GMWVD}} = \{q \in \mathcal{F} \mid \frac{d(q, p_{ii}) + \epsilon_{ii}}{r_i} \leq \frac{d(q, p_{ij}) - \epsilon_{ij}}{r_j}\}. \quad (4)$$

A special case of this approach, in which  $\epsilon_{ii} = 0$  has recently been studied in [13].

#### 2) Guaranteed Power Diagram (GPD):

$$\Pi_i^{\text{GPD}} = \{q \in \mathcal{F} \mid [d(q, p_{ii}) + \epsilon_{ii}]^2 - r_i^2 \leq [d(q, p_{ij}) - \epsilon_{ij}]^2 - r_j^2\}. \quad (5)$$

*Remark 2.* One special case of the above diagrams is the case where  $\epsilon_{ii} = 0$  which implies that  $p_{ii} = p_i$ . That is, each sensor knows or is able to measure its own position accurately. This is practically important, e.g., in GPS-equipped sensors [10] and can be studied per se, too.

### B. Regions' Properties

It is now straightforward to see that Proposition 1 is valid for any of the above guaranteed regions. In addition, we have

**Proposition 2.** *The regions defined by (4)–(5) are disjoint.*

*Proof:* On the one hand, one can verify that  $\Pi_i^{\text{GMWVD}} \subseteq \Pi_i^{\text{MWVD}}$  and  $\Pi_i^{\text{GPD}} \subseteq \Pi_i^{\text{PD}}$ . On the other hand, we know that the regions corresponding to the MWVD and PD defined by (2)–(3) are mutually disjoint. Therefore, their subsets are also disjoint.

In addition, it is worth mentioning that the regions generated by the above diagrams do not partition the field. That is, there are some *neutral areas* in the field which do not belong to any of the guaranteed regions. Mathematically,  $\bigcup_{i=1}^n \Pi_i \neq \mathcal{F}$  for the GMWVD and GPD. However, the total area of the regions which are not assigned to any sensors is not comparable to the assigned regions, if  $\epsilon_{ij}$ ,  $i, j \in \mathcal{N}$ , are relatively small. What is more, it should be highlighted that the neutral areas are not necessarily coverage holes; they might be covered with one or more sensors. Examples of the above-mentioned guaranteed diagrams are shown in Fig. 1

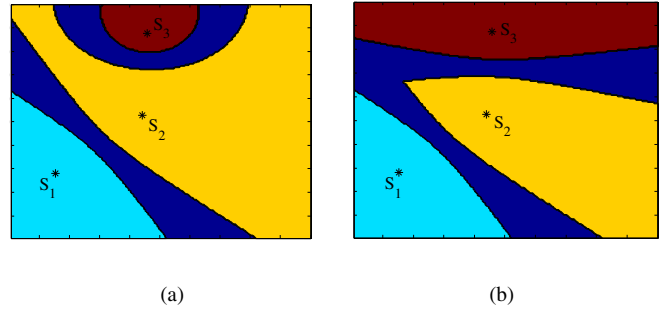


Fig. 1. Examples of guaranteed diagrams for a field containing 3 sensors with different sensing radii and imperfect location information. The dark blue regions show the areas which are not assigned to any sensor, meaning that a single-cell-based coverage hole detection is not applicable to them. (a) Guaranteed multiplicatively weighted Voronoi diagram (GMWVD). (b) Guaranteed power diagram (GPD).

We proved that the regions corresponding to the sensors are disjoint in both guaranteed diagrams. On the other hand, as we discuss in details in Section IV, the deployment algorithms are such that each sensor can move only inside its associated region. Hence, if the sensor corresponding to each region is inside that region inter-sensor collision avoidance is guaranteed.<sup>2</sup>

## IV. DEPLOYMENT PROTOCOLS

In this part different deployment protocols are developed for a network of mobile sensors with non-identical sensing ranges subject to inaccurate locations information. To this end, we use existing movement strategies, e.g., farthest point method [9], and apply them to the proposed guaranteed diagrams.

### A. Deployment Algorithm Details

The proposed deployment algorithms are iterative, and in each iteration the following steps are carried out:

- i) All sensors broadcast their sensing radii and positions. Thus, based on the received information, every sensor constructs its own region, given a guaranteed diagram.
- ii) Every sensor detects coverage holes in its own region in a distributed manner (i.e., independently).
- iii) After discovering the coverage holes, by using a specific movement algorithm (which will be discussed in subsection IV-B), the corresponding sensor calculates its new candidate location.
- iv) Once the new location is calculated, the corresponding coverage area is evaluated (based on the previously-constructed region) and compared to the current coverage area. The sensor moves to the new location only if the resulting coverage area is greater than the present value; otherwise, it does not move in this iteration.
- v) To have a termination criterion for the algorithm, a proper threshold  $\delta$  is defined; the algorithm is terminated if no

<sup>2</sup>Collision avoidance plays an important role in the context of managing multiple vehicles, including mobile sensor networks.

sensor can improve its coverage area by this threshold or a predefined number of iterations ( $I_{\max}$ ) has been completed.

### B. Movement Strategies

In this subsection, we describe the movement strategies applied for sensor deployment in this paper. Remember that a movement strategy is required in step iii of the above iterative algorithm to find a new candidate point (position) for each sensor. We use the following movement strategies in our work.

1) *Farthest Point (FP) Strategy*: The main idea behind this strategy is to move every sensor to the farthest point in its region such that the area of coverage hole is decreased. If the sensor  $s_i$  detects a coverage hole in its corresponding region, it calculates the farthest point in that region, and moves toward it until this point is covered.

2) *Minmax Point (MP) Strategy*: There are certain network topologies and sensor configurations for which the FP strategy is not very effective. Examples of such regions are shown in [14], in which usually the angle is narrow, and thus if the sensor moves there the local coverage (i.e., coverage in the cell) decreases. Under such a situation the algorithm forces the sensor to remain in its previous location while it was still possible to improve the local coverage if the sensor was properly placed in the region.

The minmax point (MP) strategy is proposed in the sequel to address this shortcoming of the FP strategy. The main idea behind the MP strategy is that to achieve maximum coverage, no sensor should be too far from any point in its corresponding region. The MP strategy considers the candidate position for each sensor as a location inside the corresponding region whose distance from the farthest point of the region is minimum. This may yield a better coverage compared to the one obtained by using the FP technique.

The above movement strategies can be used in combination with the diagrams we introduced in Section III. Specifically, the following deployment algorithms are possible if the FP strategy is used for movement (step iii of the above iterative algorithm).

- Farthest point based GMWVD (FPGMW)
- Farthest point based GPVD (FPGP)

Similarly, one can use the MP movement strategy in each of the diagrams to get MPGMW and MPGP deployment algorithms. We compare the performance of these algorithms for various number of sensors in the next section.

## V. SIMULATION RESULTS

We evaluate the performance of the proposed algorithms by performing simulations for different number of sensors in a  $50m \times 50m$  field. The results presented in this section are obtained by using 20 random initial arrangements for the sensors. The coverage improvement threshold  $\delta$  is set to be  $0.1m^2$ , meaning that if the local coverage (i.e., coverage in a cell) improvement by all sensors is less than  $0.1m^2$ , the algorithm stops. There are three types of sensors with sensing radii equal to 6m, 6.5m and 7m. The value of  $\epsilon_{ij}$  is set to be 0, i.e., we assume each sensor knows its exact location,

whereas  $\epsilon_{ij} = 0.1m$  for all nodes. We consider four different number of sensors, namely,  $n = 18, 27, 36, 45$ . Table I shows the number of sensors from each type for different  $n$ . For each setting, we carry out simulation for different algorithms which are the FPGMW, FPGP, MPGMW, and MPGP.

TABLE I  
THE DISTRIBUTION OF SENSORS WITH DIFFERENT RADII FOR EACH  $n$ .

	$r = 6m$	$r = 6.5m$	$r = 7m$
$n = 18$	10	6	2
$n = 27$	15	9	3
$n = 36$	20	12	4
$n = 45$	25	15	5

Total sensing coverage of the field, after certain number of iterations, is the first parameter we are interested in. Fig. 2 represents the coverage factor of the sensor network (defined as the ratio of the covered area to the overall area) for each algorithm at various iterations when 36 sensors are deployed. It can be seen that the coverage is sharply increasing for the first few iterations and after several iterations the coverage remains almost constant. Specifically, the coverage goes from less than 80% up to more than 96% just in five iterations, for the MPGMW and MPGP algorithms. We are not including the coverage plots for  $n = 18, 27, 45$ , due to the space limit and similarity of their behavior to the case with  $n = 36$ . Obviously, the sensing coverage depends on the number of sensors and it increases when  $n$  goes up. To visualize this, in Fig. 3 we plot the initial and final coverage factor versus the number of sensors for each of the proposed deployment algorithms.

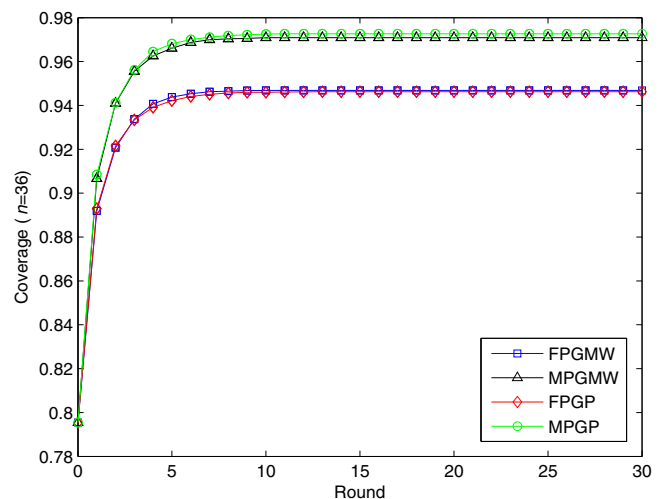


Fig. 2. Network coverage for 36 sensors using different algorithms at various iterations.

Overall, the coverage provided by the MP-based algorithms is larger than that of the FP-based algorithms. This

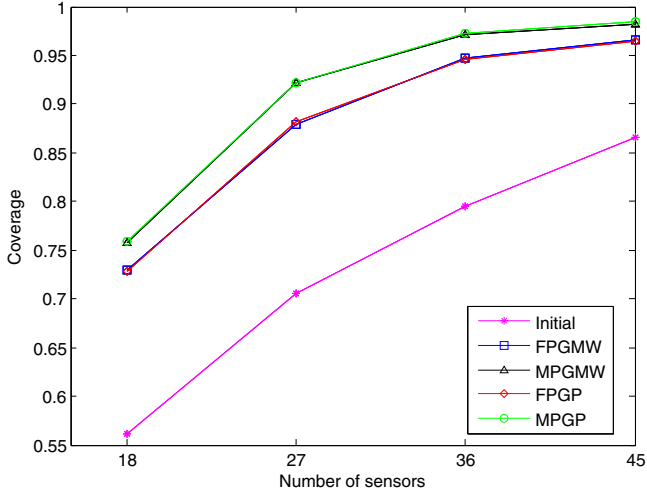


Fig. 3. Network coverage versus number of sensors for different algorithms.

is, however, achieved at the expense of a larger number of movements and travel distances for the sensors, as represented in Fig. 4 and Fig. 5, respectively. The latter two parameters are sensible indicators of energy consumptions caused by sensor movements [14]. Fig. 4 indicates that the average moving distance per sensor, required to cover the field, decreases as the number of sensors increases. This makes sense since the higher the number of sensors, the better the initial coverage and thus fewer movements are needed to improve the coverage.

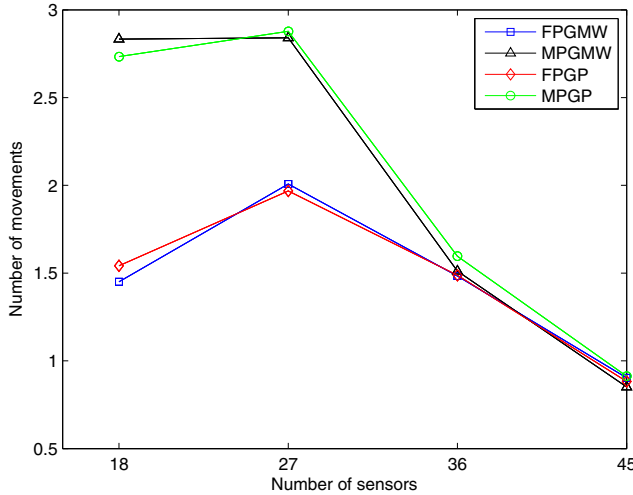


Fig. 4. Number of movements required to reach the termination condition using the proposed algorithms with different number of sensors.

In general, there is only little difference in the performance of the MP-based algorithms, in terms of coverage, average moving distance, and average number of movements to achieve a certain level of coverage. A similar pattern

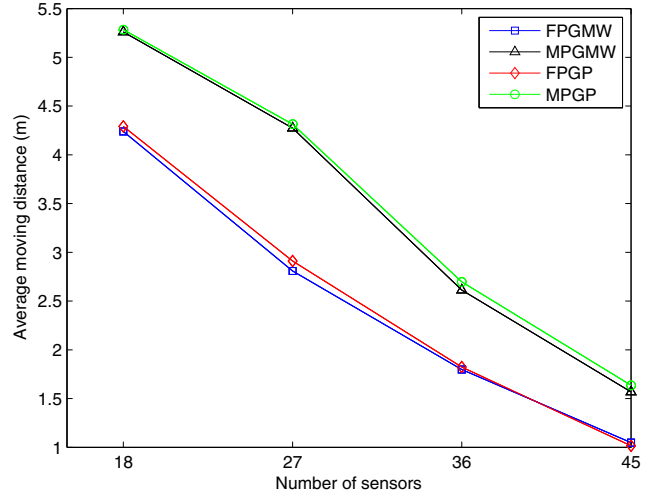


Fig. 5. Average travel distance per sensor for the proposed algorithms given different number of sensors in the field.

is observed for the FP-based algorithms. In other words, although the structures of cells in the GMWVD and GPD are somewhat different, this does not have much effect on the performance of the sensor deployment algorithms. In contrast, the movement strategy, i.e. the FP or MP, is more determinant, as for a given diagram (e.g., the GP diagram), the performance of the deployment algorithms, in various senses, is noticeably different for the MP and FP, as it is evident from Figs. 2–5.

It is also instructive to have a sense of the number of iterations required to terminate each algorithm. This is shown in Fig. 6 in which, except for  $n = 18$ , the number of iteration required to reach a steady state (i.e., to terminate the algorithm since there is not more improvement) decreases as the number of sensors goes up. This makes sense, since with higher number of sensors the initial coverage is higher and it takes less time (iterations) to reach the steady state. However, when the number of sensors is very small to cover the field, the average number of movements and the number of iterations become smaller, possibly because initial distribution of sensors is such that they do not overlap much. To better understand this, consider the extreme case where there is only one sensor in the field. Then, it is clear that if the sensing area of the sensor is completely inside the field, the coverage cannot be improved anymore and thus the sensor does not need any movement; further, the number of iterations in the deployment algorithm will be 0. If the sensing area of the sensor is partially out of the field, the system can reach its best performance just in one movement and at the first iteration. In light of Fig. 6, and Fig. 4, it can be concluded that 18 sensors are not enough to effectively cover the field.

Finally, we investigate the effect of the magnitude of error on the coverage performance. Table II presents the coverage results for the FPGMW algorithm. Intriguingly, the system

TABLE II

THE FINAL COVERAGE PERCENTAGE FOR DIFFERENT MEASUREMENT ERRORS BASED ON THE FPGMW ALGORITHM WITH  $\epsilon_{ii} = 0.1m$ .

	Exact information	$\epsilon_{ij} = 0.1m$	$\epsilon_{ij} = 0.25m$	$\epsilon_{ij} = 0.5m$	$\epsilon_{ij} = 0.75m$	$\epsilon_{ij} = 1m$	$\epsilon_{ij} = 1.5m$
$n = 18$	72.61%	72.12%	72.03%	73.13%	73.30%	73.06%	72.14%
$n = 27$	89.30%	89.79%	90.02%	89.11%	88.42%	87.40%	85.88%
$n = 36$	97.16%	97.26%	96.85%	96.10%	95.03%	94.07%	92.37%
$n = 45$	97.84%	97.92%	97.91%	97.3%	96.82%	96.23%	94.36%

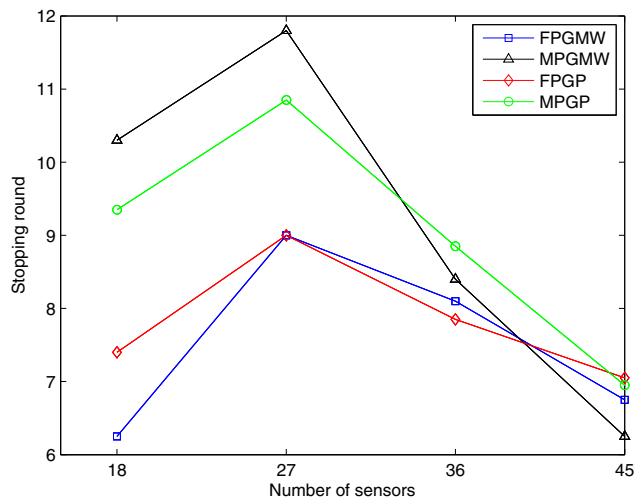


Fig. 6. Average number of iterations used to meet the termination condition in different algorithms, for 18, 27, 36, and 45 sensors in the field.

performance can be improved if the error is increased to a certain extent, depending on the number of sensors in the field. For example, from Table II one can see that for  $n = 18$  if  $\epsilon_{ij}$  goes from 0 up to  $0.75m$ , the coverage increases. For this specific case, the best result is achieved for  $\epsilon_{ij} = 0.75m$  which is relatively high error. When the number of sensors increases the best performance is attained for smaller error magnitudes. However, for any  $n$  the performance with some mild errors is better than that for the based on the exact information where  $\epsilon_{ij} = 0$  and  $\epsilon_{ii} = 0$ . This indicates that even if the locations of sensors are exactly known at each node, it is recommended to add some random but bounded errors to that information and exploit the proposed guaranteed Voronoi-based diagrams to improve the system performance. The amount of error to be added may depend on other parameters such as the density of sensors in the field and is subject to further studies.

## VI. CONCLUSIONS

To increase the sensing coverage in a network of mobile sensors with non-identical sensing radii and in the presence of location measurement errors, we have proposed Voronoi-based diagrams that can independently search for the coverage holes in each cell. We have then used two movement strategies, namely, the farthest point and minmax point, within the cells developed by the proposed diagrams to relocate the sensors in order to increase the networks sensing

coverage. Numerical results, with inaccurate location information, show that the proposed algorithms can effectively increase the network coverage. Intriguingly, even if sensors location information are exact, using the proposed algorithms can improve the network coverage when compared to the existing algorithms which are developed based on the exact location information.

## REFERENCES

- [1] G. Wang, G. Cao, and T. La Porta, "Movement-assisted sensor deployment," *IEEE Transactions on Mobile Computing*, vol. 5, no. 6, pp. 640–652, 2006.
- [2] S. Megerian, F. Koushanfar, M. Potkonjak, and M. B. Srivastava, "Worst and best-case coverage in sensor networks," *IEEE Transactions on Mobile Computing*, vol. 4, no. 1, pp. 84–92, 2005.
- [3] Q. Du, V. Faber, and M. Gunzburger, "Centroidal Voronoi tessellations: Applications and algorithms," *SIAM review*, vol. 41, no. 4, pp. 637–676, 1999.
- [4] J. Cortes, S. Martinez, T. Karatas, and F. Bullo, "Coverage control for mobile sensing networks," in *Proc. IEEE International Conference on Robotics and Automation (ICRA)*, vol. 2, pp. 1327–1332, 2002.
- [5] S. He, J. Chen, and Y. Sun, "Coverage and connectivity in duty-cycled wireless sensor networks for event monitoring," *IEEE Transactions on Parallel and Distributed Systems*, vol. 23, no. 3, pp. 475–482, 2012.
- [6] M. Ma and Y. Yang, "Adaptive triangular deployment algorithm for unattended mobile sensor networks," *IEEE Transactions on Computers*, vol. 56, no. 7, pp. 946–958, 2007.
- [7] X. Wang, S. Han, Y. Wu, and X. Wang, "Coverage and energy consumption control in mobile heterogeneous wireless sensor networks," *IEEE Transactions on Automatic Control*, vol. 58, no. 4, pp. 975–988, 2013.
- [8] S. Yang, M. Li, and J. Wu, "Scan-based movement-assisted sensor deployment methods in wireless sensor networks," *IEEE Transactions on Parallel and Distributed Systems*, vol. 18, no. 8, pp. 1108–1121, 2007.
- [9] H. Mahboubi, K. Moezzi, A. G. Aghdam, K. Sayrafian-Pour, and V. Marbukh, "Self-deployment algorithms for coverage problem in a network of mobile sensors with unidentical sensing range," in *Proceedings of IEEE Global Communications Conference*, pp. 1–6, 2010.
- [10] G. Han, H. Xu, T. Q. Duong, J. Jiang, and T. Hara, "Localization algorithms of wireless sensor networks: a survey," *Telecommunication Systems*, vol. 52, no. 4, pp. 2419–2436, 2013.
- [11] E. Deza and M. M. Deza, *Encyclopedia of Distances*. Springer, 2009.
- [12] F. Aurenhammer, "Voronoi diagrams a survey of a fundamental geometric data structure," *IEEE Transactions on Automatic Control*, vol. 23, no. 3, pp. 345–405, 1991.
- [13] F. Sharifi, Y. Zhang, and A. Aghdam, "A distributed deployment strategy for multi-agent systems subject to health degradation and communication delays," *Journal of Intelligent & Robotic Systems*, vol. 73, no. 1-4, pp. 623–633, 2014.
- [14] H. Mahboubi, K. Moezzi, A. G. Aghdam, K. Sayrafian-Pour, and V. Marbukh, "Distributed deployment algorithms for improved coverage in a network of wireless mobile sensors," *IEEE Transactions on Industrial Informatics*, vol. 10, no. 1, pp. 163–174, 2014.